

## Depth-Average Velocity from Spray Underwater Gliders

DANIEL L. RUDNICK, JEFFREY T. SHERMAN, AND ALEXANDER P. WU

*Scripps Institution of Oceanography, La Jolla, California*

(Manuscript received 21 November 2017, in final form 18 June 2018)

### ABSTRACT

The depth-average velocity is routinely calculated using data from underwater gliders. The calculation is a dead reckoning, where the difference between the glider's velocity over ground and its velocity through water yields the water velocity averaged over the glider's dive path. Given the accuracy of global positioning system navigation and the typical 3–6-h dive cycle, the accuracy of the depth-average velocity is overwhelmingly dependent on the accurate estimation of the glider's velocity through water. The calculation of glider velocity through water for the Spray underwater glider is described. The accuracy of this calculation is addressed using a method similar to that used with shipboard acoustic Doppler current profilers, where water velocity is compared before and after turns to determine a gain to apply to glider velocity through water. Differences of this gain from an ideal value of one are used to evaluate accuracy. Sustained glider observations of several years off California and Palau consisted of missions involving repeated straight sections, producing hundreds of turns. The root-mean-square accuracy of depth-average velocity is estimated to be in the range of 0.01–0.02 m s<sup>-1</sup>, consistent with inferences from the early days of underwater glider design.

### 1. Introduction

The ocean sciences have seen increasing use of underwater gliders (Rudnick et al. 2004) to address a wide range of research (Rudnick 2016). In typical use, underwater gliders dive as deep as 1000 m, completing a cycle in 6 h and covering 6 km horizontally through water in that time. In addition to delivering profiles of such variables as temperature and salinity, underwater gliders measure horizontal velocity averaged over the depth of their profiles. The purpose of this paper is to detail how this depth-average velocity is calculated using data from Spray underwater gliders (Sherman et al. 2001) and especially to quantify the accuracy of the velocity.

Depth-average velocity has been estimated from underwater gliders of all types from their very first uses (Eriksen et al. 2001; Davis et al. 2003). This estimate is essentially a dead reckoning, where the velocity over ground during a glider's dive is differenced from its velocity through water to yield the depth-average velocity. The velocity over ground, averaged over a dive, is measured by differencing global positioning system (GPS) fixes at the beginning and end of the dive, and dividing by the dive's duration. The velocity through water is calculated using measurements of pressure,

heading, and pitch, and with knowledge of the glider's hydrodynamics. Our approach to this calculation is presented in section 2.

The accuracy of the depth-average velocity is overwhelmingly dependent on the accuracy of the glider's velocity through water. Given the root-mean-square (rms) accuracy of GPS of about 4 m (see <https://www.gps.gov/>; DoD 2008), the resulting rms accuracy of glider velocity over ground across a 6-h dive is estimated as  $\sqrt{2}(4\text{ m})/(6 \times 3600\text{ s}) = 0.0003\text{ m s}^{-1}$ . Using the accuracies of measuring glider orientation and uncertainties in hydrodynamics, early publications on gliders reported an accuracy of glider velocity through water of about 0.01 m s<sup>-1</sup> (Eriksen et al. 2001; Davis et al. 2003). Todd et al. (2011) suggested an approach to estimating this accuracy similar to that used for shipboard acoustic Doppler current profilers (ADCPs), where velocity before and after turns were analyzed. The accuracy of 0.01 m s<sup>-1</sup> was supported by Todd et al. (2011) using the first three years of data from the California Underwater Glider Network (CUGN; Rudnick et al. 2017). We revisit this analysis in section 3 with the benefit of over 10 years of data from CUGN and additional data from sustained operations off Palau. The presentation in Todd et al. (2011) was limited to less than a page in an appendix. We take this opportunity to present a complete description of our method for calculating depth-average velocity from

---

*Corresponding author:* Daniel L. Rudnick, drudnick@ucsd.edu

DOI: 10.1175/JTECH-D-17-0200.1

© 2018 American Meteorological Society. For information regarding reuse of this content and general copyright information, consult the [AMS Copyright Policy](https://www.ametsoc.org/PUBSReuseLicenses) ([www.ametsoc.org/PUBSReuseLicenses](https://www.ametsoc.org/PUBSReuseLicenses)).

Spray and a general approach to evaluating the accuracy of depth-average velocity from any type of underwater glider.

The depth-average velocity is a unique feature of the underwater glider as an oceanographic platform. Navigation of a glider depends on the depth-average velocity, either to travel between waypoints or to cross currents. Also, the depth-average velocity forms an important component of a glider's scientific value. For example, the horizontal integration of the across-track component of this depth-average velocity allows estimation of transport. The accuracy of such a transport estimate is dependent on the accuracy of depth-average velocity, as  $0.01 \text{ m s}^{-1}$  implies a transport of  $1 \text{ Sv}$  ( $10^6 \text{ m}^3 \text{ s}^{-1}$ ) over a depth of 1000 m and across a section 100 km long. Confirming this accuracy is critical to using gliders to measure oceanographically relevant currents. Observed profiles of temperature and salinity allow the calculation of geostrophic shear through along-track gradients of density. The absolute geostrophic current may then be estimated using the depth-average velocity as a reference. These geostrophic currents are important products of glider measurements, particularly given the widespread use of gliders in boundary currents.

## 2. Calculation of depth-average velocity

The calculation of glider velocity is conceptually straightforward (Fig. 1). Given the glide angle through water  $\phi$  (measured relative to the horizontal) and the glider's vertical displacement  $dz$ , the horizontal displacement  $dr$  through water is

$$dr = dz \cot \phi. \quad (1)$$

The glide angle is the sum of the glider pitch  $\phi_g$  (the direction of the glider nose relative to the horizontal) and the angle of attack  $\phi_a$  (the positive angle between pitch and the motion of the glider through water),

$$\phi = \phi_g + \phi_a \text{ sign} \phi_g, \quad (2)$$

where the sign function properly accounts for ascents and descents. Based on the hydrodynamics of Spray's wings and hull, the angle of attack is estimated to be  $3^\circ$  for a glider pitch of  $17^\circ$  (Sherman et al. 2001). A Spray underwater glider is controlled to maintain a single desired heading throughout its dive. The glider typically completes its turn to this heading within the first 50 m of descent, during which time the angle of attack may change and there may be sideslip. A purpose of this work is to validate the angle of attack and sideslip from ocean data, averaged over a complete dive.

In practice, the calculation of horizontal displacement is done over increments determined by the sampling

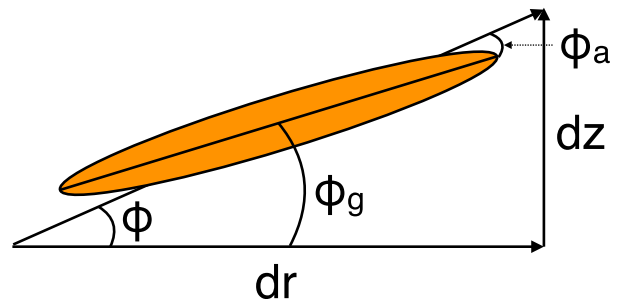


FIG. 1. A schematic diagram of glider flight, with horizontal  $dr$  and vertical  $dz$  displacements, and glide angle  $\phi$ , glider pitch  $\phi_g$ , and angle of attack  $\phi_a$ .

interval. Spray records data every 8 s during flight. The change of depth  $dz$  calculated from pressure (Fofonoff and Millard 1983) during each 8-s period is used along with measured pitch to calculate horizontal displacement through water  $dr$ . Measurements of heading  $\theta$  (relative to true north) allow the calculation of eastward  $dx$  and northward  $dy$  displacement,

$$\begin{aligned} dx &= dr \sin \theta \\ dy &= dr \cos \theta. \end{aligned} \quad (3)$$

The incremental displacements  $dr$ ,  $dx$ , and  $dy$  are summed over a complete dive cycle to yield the total displacements  $r$ ,  $x$ , and  $y$ , respectively. The sum to create total displacement starts and ends at the surface, so random error in pressure measurements must sum to zero, and any error must be due to measurements of pitch and heading, or shortcomings in the simple model of glider flight expressed in Eqs. (1)–(3). A number of corrections are made to the displacement calculation to exclude instances when the glider is near stall; these corrections are discussed in the appendix.

Examples of dives plotted as depth against time and horizontal distance through water are shown (Fig. 2) for missions off California (500-m dive) and Palau (1000-m dive). The gliders are controlled to maintain a constant pitch of  $17^\circ$ , so the path through water is a nearly perfect triangle wave. The curve for depth as a function of time is not a straight line. The glider empties its external bladder at the surface before a dive, so it descends with constant volume and necessarily slows as the seawater density increases with depth. On ascent the glider may increase volume to maintain a minimum vertical velocity, so, in general, the ascent takes less time than the descent. The time it takes to get to a given depth can be read off the blue time curve to determine how the glider travels along the black trajectory through water. Fluctuations in the depth versus time curves are the result of internal waves as the glider is heaved along with the

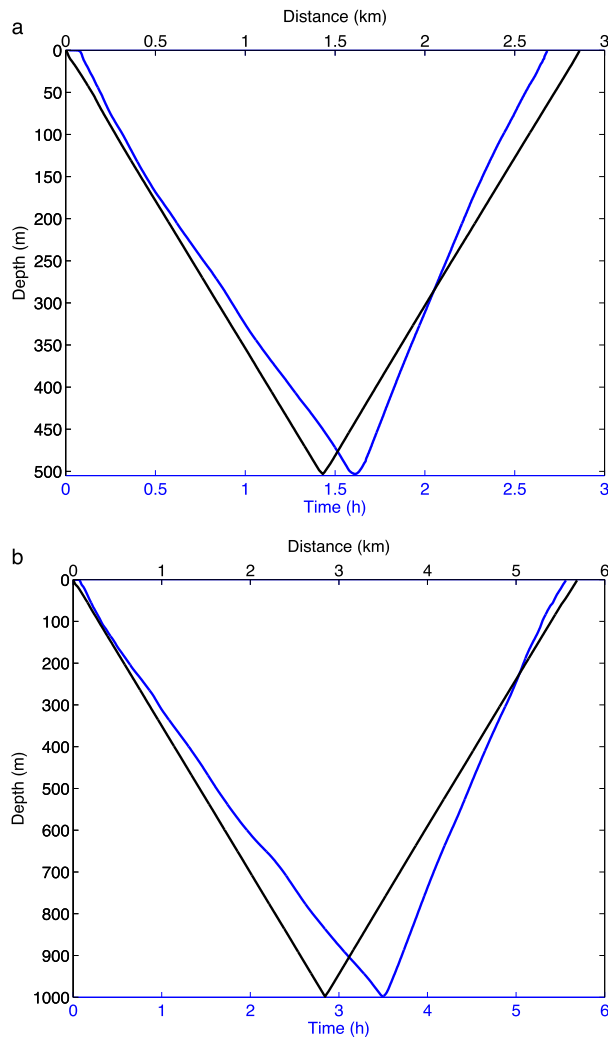


FIG. 2. Depth against time (blue) and horizontal distance through water (black) for Spray underwater glider dives off the coasts of (a) California to 500 m and (b) Palau to 1000 m. Note the difference in scales on the axes in the two panels.

wave (Rudnick et al. 2013). The depth versus horizontal distance through water curves are unchanged by internal waves, as the glider's path through water remains relatively constant. The entire dive covers nearly the same value in distance measured in kilometers as in time measured in hours, so the horizontal speed through water is approximately  $1 \text{ km h}^{-1}$  ( $0.28 \text{ m s}^{-1}$ ). The estimated speed for the California dive is  $0.29 \text{ m s}^{-1}$  and for the Palau drive  $0.28 \text{ m s}^{-1}$ . These speeds are typical of clean, recently deployed gliders.

The calculation of the depth-average water velocity proceeds as follows. The glider's velocity through water is calculated by dividing the total displacement through water by the dive cycle time. The velocity through water is actually a time average over the path the glider took

during the dive. This is approximately equivalent to a depth average because the glider's path is nearly a triangle; this approximation is examined further at the end of section 3. The depth-average water velocity  $u$  is the difference between the velocity over ground as measured by GPS fixes at the beginning and end of each dive  $u_g$  and the velocity through water  $u_r$ ,

$$u = u_g - u_r, \quad (4)$$

where we take the velocity to be a complex variable whose real part is the eastward velocity and the imaginary part is the northward velocity. The depth-average velocity is unique to gliders, as they profile continuously.

A crucial step in the preparation of a Spray underwater glider is the calibration of the compass. The Spray uses a Precision Navigation Inc. TCM2.5, with a magneto-inductive three-axis magnetometer. The effect of local magnetic anomalies near the compass (caused by steel battery cases, for example) is measured by performing a compass calibration for every deployment. The calibration involves spinning Spray on a computer-controlled table in an outside area away from stray magnetic fields over a wide range of pitch, roll, and heading. The local anomaly field vector is estimated through a least squares approach and stored on board. This first-order correction is applied directly to all three-axis magnetometer readings, significantly improving accuracy, but still leaving a typical residual rms  $1.5^\circ$  error curve. Residual error curves are measured for  $0^\circ$  and  $\pm 17^\circ$  pitches to match pitch during flight, and then applied during post-processing to improve accuracy. Magnetic declination at the glider's deployed location is added to get true heading. The changes in magnetic declination along the glider's path are addressed during processing as necessary, and models of angle of attack that depend on pitch and speed can be applied.

### 3. Quantification of the accuracy of depth-average velocity

The measurement accuracy of depth-average velocity depends on a variety of factors. First, the accuracy depends on the quality of measurements of the variables that go into the calculation—especially heading and pitch. Second, the accuracy depends on the glider having a repeatable hydrodynamic shape: wings and tail fin are true, hull is clean, and the  $3^\circ$  assumed angle of attack is correct. Third, internal waves cause changes in vertical velocity that are unrelated to the motion of the glider through the water. Fourth, biofouling can change the glider's hydrodynamic properties, including angle of attack, although we take steps to limit biofouling with

coatings when necessary. The first and second of these sets of factors are largely under our control, while the third and fourth are uncontrolled. The accuracy of  $0.01 \text{ m s}^{-1}$  for depth-average velocity from the early publications (as summarized in the introduction) were based on plausible accuracies in measuring the relevant variables on clean gliders. Any quantification of the accuracy that explicitly and separately accounts for all of these errors would have several parameters that could be reasonably questioned.

With all the potential sources of error, the best practical approach to quantify accuracy is through analyses of in situ ocean measurements. The approach presented here follows that used for decades in the calibration of shipboard ADCPs (Joyce 1989; Pollard and Read 1989; Rudnick and Luyten 1996). The basic idea is to take advantage of times when the vehicle turns, and to assume that the ocean velocity is identical before and after the turn. We assume that the error in the estimated glider through water velocity  $\hat{u}_r$  can be corrected through multiplication by a complex gain  $\gamma$ . Substituting  $\gamma\hat{u}_r$  into Eq. (4) yields

$$u = u_g - \gamma\hat{u}_r. \quad (5)$$

Equating the water velocity before and after a turn results in an equation for  $\gamma$ ,

$$\gamma = \frac{u_{g1} - u_{g2}}{\hat{u}_{r1} - \hat{u}_{r2}}, \quad (6)$$

where the subscripts refer to either side of the turn. If all measurements were perfect and ocean velocity was constant, then  $\gamma$  would be exactly one. Errors in the direction of the glider's velocity through water are evident in the phase of  $\gamma$ , and errors in the speed through water cause  $\gamma$  to have a magnitude different from one.

We evaluated  $\gamma$  from turns in our glider database (Rudnick et al. 2016), focusing on two projects off California and Palau. These projects were chosen because they involved the repeated occupation of sections, and the turns at the ends of the sections were thus ideally  $180^\circ$ . In practice, turns were never ideal, and the ocean velocity was not constant. To address ocean variability, we averaged over a day on either side of the turn to reduce the effects of tidal motions. So, for missions off California with 3-h dive cycle, we averaged velocities over eight dives on either side of the turn, and for Palau with a 6-h dive cycle, we averaged over four dives. We developed an algorithm to find turns that met the following conditions: 1) the angle between single dive displacements over ground on either side of the turn was less than  $55^\circ$ , 2) the angle between a day's displacements on either side of the turn was less than  $20^\circ$ , 3) the distance covered on either side of the turn was at least 10 km, 4) all

GPS data were good within a day of the turn, and 5) the turn was sufficiently far from the coast. The first three conditions assured the glider path on either side of the turn covered roughly the same ground. Condition 4 simply required good GPS data. Condition 5 was needed to reject turns in shallow water nearshore, where the currents vary rapidly.

An examination of typical turns off California and Palau (Fig. 3) help to understand the procedure for defining turns and calculating  $\gamma$ . The dives on which these turns are centered are the ones shown in Fig. 2. Off California, dives are to 500 m, and eight dives on either side of a turn are considered. The turn satisfies all the conditions above, so the tracks on either side are reasonably close to each other. The standard deviation of depth-average velocity during these 2 days is  $0.05 \text{ m s}^{-1}$  and is likely the result of ocean variability at shorter time scales as by tides and internal waves. Comparing the dives before and after the turn, the depth-average velocity has a magnitude of  $0.04 \text{ m s}^{-1}$  on either side of the turn with a difference in direction of  $10^\circ$ . An application of Eq. (6) yields a  $\gamma$  of magnitude 1.011 and phase  $0.50^\circ$ . In the example off Palau, the depth-average velocity has a component toward the turn strong enough to cause a noticeable difference in the length of the trajectory before and after the turn. In this case, the depth-average velocity has a magnitude of  $0.06 \text{ m s}^{-1}$  before and  $0.08 \text{ m s}^{-1}$  after the turn. In addition, the depth-average velocity veers  $21^\circ$  in the clockwise direction across the turn. The value of  $\gamma$  that would cause the depth-average velocity on either side of the turn to be equal has a magnitude of 1.013 and phase of  $3.37^\circ$ .

The results of these calculations are examined in scatterplots of  $\gamma$  for all the turns in our database. We start with California, where there are 118 missions with acceptable turns, and a total of 211 turns (Fig. 4). Most of the  $\gamma$  values cluster near one, albeit with a magnitude slightly larger than one, and a small positive imaginary component. There are two sets of outliers at strongly negative imaginary values and at small real values. The points with imaginary  $\gamma$  less than  $-0.2$  are all from a single glider (Spray serial number 25) during the years 2010–12. During 2013 Spray 25 underwent major modifications and was used in a project off the Galapagos Islands. After returning to California in 2014, the  $\gamma$  values from Spray 25 are in the large cluster near one. The large imaginary components point to misalignment, causing sideslip (as by a poorly trued tail fin or misaligned compass), but we could not identify anything in the repair records that would support any conclusion. In the final analysis, we take this set of outliers to be the result of a poorly tuned glider. The second set of outliers trends toward real values smaller than one. These

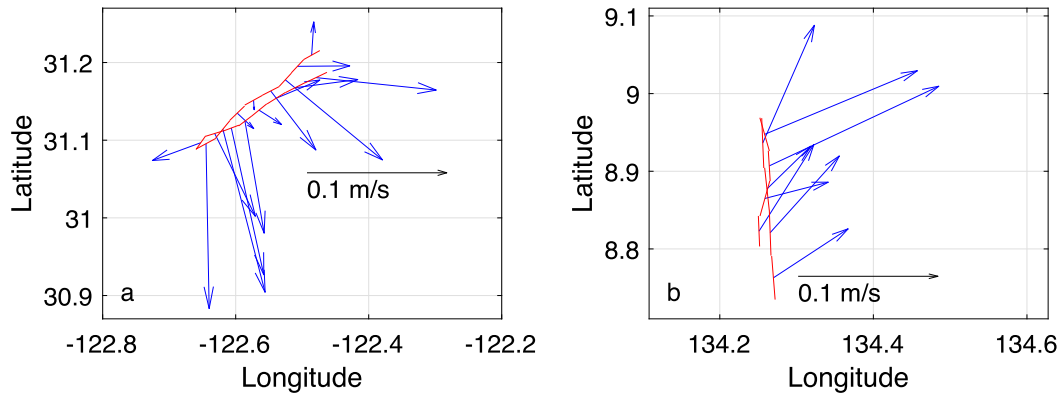


FIG. 3. Depth-average velocity during turns off (a) California and (b) Palau. The depth-average velocity is shown with blue arrows, with a scale arrow in black. Dive segments are shown in red. In each case, approximately one day of dives is shown on either side of the turn, with eight dives off California (down to 500 m) and four dives off Palau (down to 1000 m).

outliers are the result of biofouling, which increases the angle of attack. These outliers occur only on later turns during a mission and are unavoidable during the biologically productive springtime off California.

The statistics of  $\gamma$  (Table 1) provide a measure of the accuracy of glider velocity through water and therefore of depth-average velocity. The statistics are considered in four groups, either first turns only or all turns, and including or excluding the values from Spray 25 during 2010–12. The first turns are typically early during a mission before any appreciable biofouling, so the values of  $\gamma$  are indicative of a clean glider. We have reason to believe that Spray 25 was uniquely poorly aligned, so the statistics with these values excluded are more relevant to typical accuracy. Consider first the mean value of  $\gamma$ , which has a magnitude of 1.01 for first turns and 1.00 for all turns. The value for first turns suggests that our estimates of glider velocity through water need to be increased by 1%, likely because the assumed  $3^\circ$  angle of attack is too large. Taking the first-order term in the Taylor series expansion of Eq. (1) at  $20^\circ$ , the correction should be  $-0.2^\circ$ , so a refined angle of attack would be  $2.8^\circ$ . However, considering later turns, when biofouling may have an effect, the angle of attack of  $3^\circ$  seems a good choice. Considering all missions, the phase of  $\gamma$  is  $0.2^\circ$ – $0.3^\circ$ , but excluding Spray 25, the phase is  $0.8$ – $1.0^\circ$ . Ironically, the inclusion of outliers from Spray 25 yields a smaller average phase. In spite of this coincidence, we believe a better estimate of the phase bias is  $1^\circ$ , which using a mean speed through water of  $0.29 \text{ m s}^{-1}$  suggests a bias of  $0.005 \text{ m s}^{-1}$  to the right of the glider. Overall, the bias suggested by mean  $\gamma$  is negligible.

The rms deviations of  $\gamma$  yield reasonable estimates of the accuracy of glider velocity through water and

therefore of depth-average velocity. The statistics in Table 1 include the standard deviation of  $\gamma$  around the mean and rms  $\gamma - 1$  to include the error caused by the small bias. The most relevant statistics are those excluding Spray 25, for which rms values are about 0.04 for first turns and 0.06 for all turns. Multiplying by the average velocity through water yields measures of accuracy of  $0.014 \text{ m s}^{-1}$  for first turns and  $0.018 \text{ m s}^{-1}$  for all turns. These values are in reasonable agreement with the  $0.01 \text{ m s}^{-1}$  accuracy suggested by earlier publications. The degrading of accuracy later in the mission is almost certainly a result of biofouling.

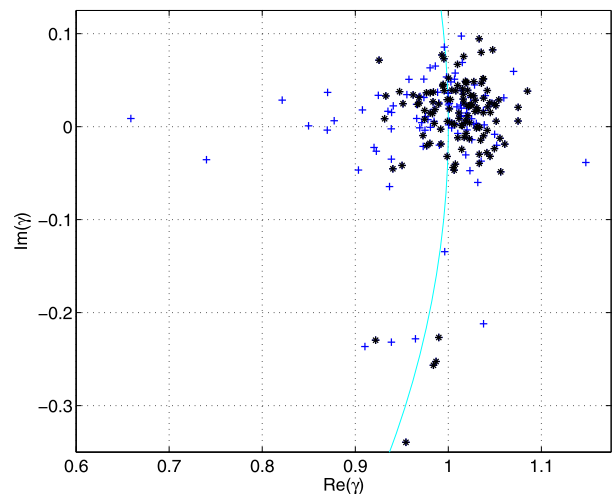


FIG. 4. A scatterplot of the real and imaginary parts of  $\gamma$  as defined in Eq. (6) for turns off California. Black asterisks are the first turns for each mission, and blue crosses are subsequent turns. The cyan curve is the unit circle. A perfectly tuned glider in an ocean with steady flow would have  $\gamma = 1$ .



TABLE 1. Statistics of  $\gamma$  [Eq. (6)] for California missions. The total error is the product of rms  $\gamma - 1$  and  $|\hat{u}_r|$ .

	All missions		Excluding Spray 25, 2010–12	
	First turns	All turns	First turns	All turns
Mean $\gamma$ (amplitude, phase)	1.010, 0.3°	0.998, 0.2°	1.012, 1.0°	0.999, 0.8°
Standard deviation $\gamma$	0.072	0.081	0.043	0.061
Root-mean-square $\gamma - 1$	0.073	0.081	0.048	0.063
Mean $ \hat{u}_r $ ( $\text{m s}^{-1}$ )	0.295	0.290	0.295	0.290
Total error ( $\text{m s}^{-1}$ )	0.021	0.023	0.014	0.018

The database includes 11 missions off Palau with 138 turns (Fig. 5). Palau has many more turns per mission, as the sections being repeated are much shorter than those off California. The values for  $\gamma$  cluster nicely around one, with outliers extending toward small  $\gamma$  as a result of biofouling. Mean  $\gamma$  off Palau is in reasonable agreement with California at magnitudes of 1.01 for first turns and 0.99 overall, and phases of about 1° (Table 2). The rms deviations of  $\gamma$  off Palau are nearly identical to those off California, and the overall accuracy is  $0.014 \text{ m s}^{-1}$  for first turns and  $0.016 \text{ m s}^{-1}$  for all turns. The agreement between the California and Palau missions supports the notion that these accuracies are generally plausible.

It is informative to compare accuracies of glider attitude sensors and angle-of-attack estimates to the  $\gamma$  statistics. According to the manufacturer of the attitude sensor, the accuracy of the pitch angle is  $0.4^\circ$ , repeatable to  $0.3^\circ$ , and the heading accuracy is  $1.5^\circ$  rms (agreeing with our correction curves), repeatable to  $0.3^\circ$ . Numerical modeling (Jenkins et al. 2003) estimates an angle-of-attack  $\phi_a$  range of  $3.0^\circ$ – $2.5^\circ$  for a pitch range of  $16^\circ$ – $20^\circ$ . The rms  $\gamma$  of about 0.04 is roughly equally partitioned between the real and imaginary parts of  $\gamma$ , so each is about 0.03. This corresponds to an rms heading accuracy of  $1.7^\circ$  and an rms pitch accuracy of  $0.6^\circ$ . These tend to be on the high side of sensor accuracies,

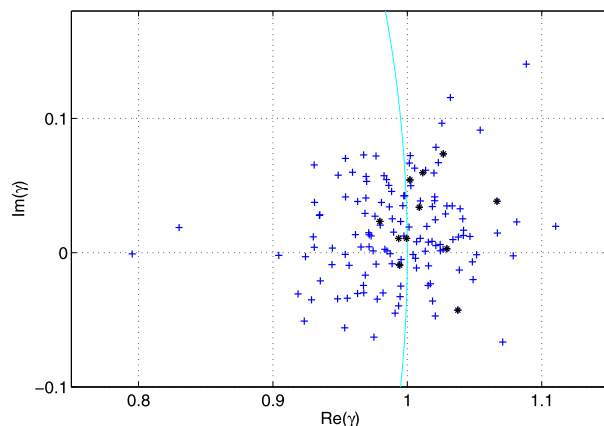


FIG. 5. As in Fig. 4, but for Palau.

consistent with a contribution of oceanic variability to accuracies possible in the laboratory.

The calculation of velocity in Eqs. (1)–(4), along the glider’s path during a dive, is averaged over time. The nearly triangle shape of glider dives (Fig. 2) supports the interpretation of this time average as equivalent to a depth average. However, systematic biases in gliders’ vertical velocity through water cause differences from an exact depth average. For Spray gliders, vertical velocity near the surface is slightly faster than near the bottom of dives, so less time is spent near the surface than at depth. To quantify this effect, we calculate the absolute value of vertical velocity in 10-m-depth bins for all dives. The inverse of vertical velocity is normalized by its mean value for each dive, and then averaged over all dives for California and Palau (Fig. 6). The resulting curves have depth averages of one and are the weighting as a function of depth that is produced by a time average.

The difference between a depth average and a time average on a glider depends on the shape of the velocity profile. For a uniform velocity profile, there is no difference between a depth average and a time average. If a vertical profile of horizontal velocity projects onto a weighting function in Fig. 6, then a difference could occur. Because the weighting is typically within a few percent of one, a top-to-bottom shear on the order of  $1 \text{ m s}^{-1}$  is required to produce an error of order  $0.01 \text{ m s}^{-1}$ . Most of the gliders used off California and Palau carried ADCPs (Todd et al. 2017), yielding the vertical shear of horizontal velocity. These shear profiles are integrated using the weightings (Fig. 6) to determine the differences between depth and time averages. The standard deviation of the differences between depth

TABLE 2. Statistics of  $\gamma$  [Eq. (6)] for Palau missions. The total error is the product of rms  $\gamma - 1$  and  $|\hat{u}_r|$ .

	First turns	All turns
Mean $\gamma$ (amplitude, phase)	1.014, 1.3°	0.994, 0.9°
Standard deviation $\gamma$	0.042	0.057
Root-mean-square $\gamma - 1$	0.050	0.060
Mean $ \hat{u}_r $ ( $\text{m s}^{-1}$ )	0.277	0.269
Total error ( $\text{m s}^{-1}$ )	0.014	0.016

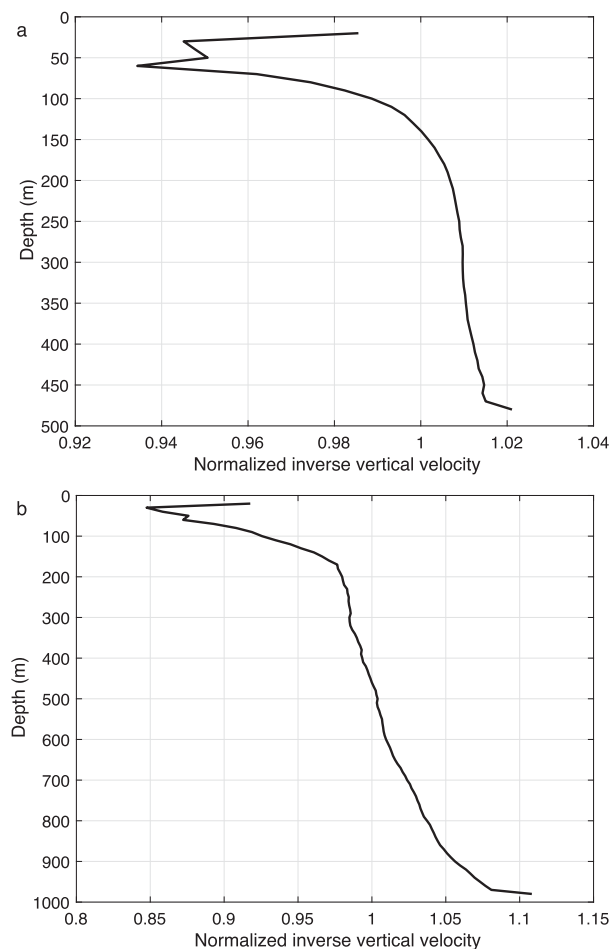


FIG. 6. Normalized inverse vertical velocity averaged over all missions from (a) California and (b) Palau. These functions are the weighting of depth-dependent velocity accomplished by time averages following typical glider paths. Note the difference in scales on the axes in the two panels.

and time averages of horizontal velocity is  $0.0015 \text{ m s}^{-1}$  for California and  $0.0044 \text{ m s}^{-1}$  for Palau. Thus, the difference between the time average along a glider path and a depth average is relatively small.

#### 4. Discussion

The calculation of  $\gamma$  for a given turn using Eq. (6) is relatively straightforward. In practice, we found the automatic identification of turns to be the most challenging part of the calculation. This automatic algorithm was checked by visual inspection of each turn. The parameters chosen to identify turns might be considered ad hoc; however, the algorithm is perfectly repeatable and could be applied to any glider in any location. Importantly, the turn-identifying algorithm depends only on the course made by the glider and not on any estimates of velocity. A

very badly fouled glider may become incapable of following a desired track, so its turns may not always be identified. It is thus reasonable to take the results presented here as relevant to clean or moderately fouled gliders.

Some of the spread in  $\gamma$  must be attributed to real variability in ocean currents over the course of the glider's turn. Our approach to addressing the high-frequency part of this variability was to calculate  $\gamma$  from averages over a day. The remaining variability is lower frequency, but it can be substantial. In particular, we examined the turns that produced the largest values of  $\gamma$ , which would suggest gliders that were especially—perhaps implausibly—slippery and fast. These turns were found often to be in strong eddies, as evidenced by ocean current and isopycnal elevations. There is reason to take the accuracies reported here as something of an upper bound.

A fair question is whether to use the  $\gamma$  calculated here to correct the velocities estimated from gliders. For example, the correction of Spray 25 during 2010–12 may make sense, as this is a single glider during a defined time, with clear characteristics. Such a correction would involve a rotation of glider velocity through water clockwise by  $14^\circ$ , and it would put the resulting values of  $\gamma$  inside the cluster from other missions. A bolder approach might be to correct the approximately  $1^\circ$  sideslip apparent over all other California and Palau missions. Such a correction would add about  $0.005 \text{ m s}^{-1}$  to the left of the glider's velocity through water. To date, we have not taken the step of using  $\gamma$  as a calibration, preferring instead to use  $\gamma$  only to evaluate accuracy.

The notion of analyzing ocean sensors in situ to establish accuracies and calibrations is well established. Such corrections include those applied to shipboard ADCPs (Joyce 1989; Pollard and Read 1989; Rudnick and Luyten 1996) and to conductivity–temperature–depth (CTD) instruments (Giles and McDougall 1986; Ochoa 1989; Lueck and Picklo 1990; Morison et al. 1994). A common calibration approach for ADCPs and CTDs is to use in situ observations without requiring special knowledge of the details of the sensor function. The resultant calibration includes all sources of sensor error as used in the field. Our approach with depth-average velocity from gliders follows the same tradition, where we produce a total accuracy regardless of the details of sensors involved and glider hydrodynamics. Because this is a total accuracy, it can be applied to glider types other than Spray such as Seaglider (Eriksen et al. 2001) and Slocum (Merckelbach et al. 2010), which use their own approaches to calculate depth-average velocity.

A fair question is whether there are methods of quantifying the accuracy of depth-average velocity that depend on accepted standards. For CTDs in particular, there are extremely accurate laboratory calibrations

that are routine and essential. Such a controlled calibration for a glider's velocity through water would ideally require a volume of still water at least 1000 m deep and 6 km long. There are lakes of sufficient size, but it is impractical to do such a calibration for every glider deployed. Another approach to calibration might be to have the glider profile near a mooring equipped with current meters capable of measuring sufficiently densely in the upper 1000 m to create a depth-average velocity. Such moorings are not commonly deployed everywhere one might want to use a glider, so an independent method to quantify accuracy, as in this paper, is needed. An example of a comparison between a glider and a mooring is presented in Todd et al. (2009).

## 5. Conclusions

The purpose of this work is to address questions about the accuracy of depth-average velocity from Spray gliders. This depth-average velocity is unique to gliders as continuously profiling platforms and is essential to using gliders to measure ocean currents. Averaging across California and Palau missions, the rms error in depth-average velocity for a freshly deployed glider is  $0.014 \text{ m s}^{-1}$ , increasing to  $0.017 \text{ m s}^{-1}$  over the course of a mission, caused by moderate biofouling. The accuracy of badly fouled gliders is essentially beyond measure, as they can become uncontrollable. We believe these accuracies are generally possible with hydrodynamically aligned gliders with well-calibrated compasses so that other glider operators may be able to reproduce the performance demonstrated by Spray.

*Acknowledgments.* The Instrument Development Group at Scripps Institution of Oceanography is responsible for Spray operations, including Ben Reineman, Evan Randall-Goodwin, Derek Vana, and Kyle Grindley. We gratefully acknowledge the support of the National Oceanic and Atmospheric Administration Ocean Observing and Monitoring Division for the California Underwater Glider Network (Grants NA15OAR4320071 and NA10OAR4320156) and the Office of Naval Research for glider operations off Palau (Grant N00014-15-1-2488). Data from Spray underwater gliders are available online ([spraydata.ucsd.edu](http://spraydata.ucsd.edu); <https://doi.org/10.21238/S8SPRAY1618>).

## APPENDIX

### Corrections Used in Calculating Depth-Average Velocity

The calculation of depth-average velocity as expressed in Eqs. (1)–(4) is relatively straightforward. In practice,

a number of corrections are made. These include the following:

- 1) Changes in depth greater than 5 m during an 8-s sample are excluded to limit the effects of strong internal waves.
- 2) The glider may sometimes back off the surface during the first 10 m of the dive; these times are excluded.
- 3) The glider may slow to near stall at the bottom of the turn, so times when vertical velocity is less than  $0.01 \text{ m s}^{-1}$  within 20 m of the bottom turn are excluded.
- 4) For very short times near the surface and bottom, as the glider is turning, the pitch may become less than  $12^\circ$ . At these times the pitch in the calculation is set to  $12^\circ$  to exclude unreasonably large velocities through water.
- 5) It takes about 60 s for the glider to roll the wing up to get a GPS fix at the beginning and end of a dive; a correction for surface velocity during this time is made.

These corrections are small relative to the errors in velocity through water. While they have little effect on the final calculation of depth-average velocity, they do correct biases. The corrections are included here for completeness.

## REFERENCES

- Davis, R. E., C. C. Eriksen, and C. P. Jones, 2003: Autonomous buoyancy-driven underwater gliders. *Technology and Applications of Autonomous Underwater Vehicles*, G. Griffiths, Ed., Taylor and Francis, 37–58.
- DoD, 2008: Global Positioning System Standard Positioning Service performance standard. 4th ed. U.S. Department of Defense Doc., 160 pp.
- Eriksen, C. C., T. J. Osse, R. D. Light, T. Wen, T. W. Lehman, P. L. Sabin, J. W. Ballard, and A. M. Chiodi, 2001: Seaglider: A long-range autonomous underwater vehicle for oceanographic research. *IEEE J. Oceanic Eng.*, **26**, 424–436, <https://doi.org/10.1109/48.972073>.
- Fofonoff, N. P., and R. C. Millard, 1983: Algorithms for computations of fundamental properties of seawater. UNESCO Tech. Papers in Marine Science 44, 53 pp.
- Giles, A. B., and T. J. McDougall, 1986: Two methods for the reduction of salinity spiking of CTDs. *Deep-Sea Res.*, **33A**, 1253–1274, [https://doi.org/10.1016/0198-0149\(86\)90023-3](https://doi.org/10.1016/0198-0149(86)90023-3).
- Jenkins, S. A., and Coauthors, 2003: Underwater glider system study. University of California, San Diego, Scripps Institution of Oceanography, 242 pp., <https://escholarship.org/uc/item/1c28t6bb>.
- Joyce, T. M., 1989: On in situ “calibration” of shipboard ADCPs. *J. Atmos. Oceanic Technol.*, **6**, 169–172, [https://doi.org/10.1175/1520-0426\(1989\)006<0169:OISOSA>2.0.CO;2](https://doi.org/10.1175/1520-0426(1989)006<0169:OISOSA>2.0.CO;2).
- Lueck, R. G., and J. J. Picklo, 1990: Thermal inertia of conductivity cells: Observations with a Sea-Bird cell. *J. Atmos. Oceanic Technol.*, **7**, 756–768, [https://doi.org/10.1175/1520-0426\(1990\)007<0756:TIOCCO>2.0.CO;2](https://doi.org/10.1175/1520-0426(1990)007<0756:TIOCCO>2.0.CO;2).



- Merckelbach, L., D. Smeed, and G. Griffiths, 2010: Vertical water velocities from underwater gliders. *J. Atmos. Oceanic Technol.*, **27**, 547–563, <https://doi.org/10.1175/2009JTECHO710.1>.
- Morison, J., R. Andersen, N. Larson, E. D'Asaro, and T. Boyd, 1994: The correction for thermal-lag effects in Sea-Bird CTD data. *J. Atmos. Oceanic Technol.*, **11**, 1151–1164, [https://doi.org/10.1175/1520-0426\(1994\)011<1151:TCFTLE>2.0.CO;2](https://doi.org/10.1175/1520-0426(1994)011<1151:TCFTLE>2.0.CO;2).
- Ochoa, J., 1989: A practical determination of CTD platinum resistance thermometer response time, and its use to correct salinity bias and spikes. *Deep-Sea Res.*, **36A**, 139–148, [https://doi.org/10.1016/0198-0149\(89\)90023-X](https://doi.org/10.1016/0198-0149(89)90023-X).
- Pollard, R., and J. Read, 1989: A method for calibrating shipmounted acoustic Doppler profilers and the limitations of gyro compasses. *J. Atmos. Oceanic Technol.*, **6**, 859–865, [https://doi.org/10.1175/1520-0426\(1989\)006<0859:AMFCSA>2.0.CO;2](https://doi.org/10.1175/1520-0426(1989)006<0859:AMFCSA>2.0.CO;2).
- Rudnick, D. L., 2016: Ocean research enabled by underwater gliders. *Annu. Rev. Mar. Sci.*, **8**, 519–541, <https://doi.org/10.1146/annurev-marine-122414-033913>.
- , and J. R. Luyten, 1996: Intensive surveys of the Azores Front. 1. Tracers and dynamics. *J. Geophys. Res.*, **101**, 923–939, <https://doi.org/10.1029/95JC02867>.
- , R. E. Davis, C. C. Eriksen, D. M. Fratantoni, and M. J. Perry, 2004: Underwater gliders for ocean research. *Mar. Technol. Soc. J.*, **38**, 73–84, <https://doi.org/10.4031/002533204787522703>.
- , T. M. S. Johnston, and J. T. Sherman, 2013: High-frequency internal waves near the Luzon Strait observed by underwater gliders. *J. Geophys. Res. Oceans*, **118**, 774–784, <https://doi.org/10.1002/jgrc.20083>.
- , R. E. Davis, and J. T. Sherman, 2016: Spray underwater glider operations. *J. Atmos. Oceanic Technol.*, **33**, 1113–1122, <https://doi.org/10.1175/JTECH-D-15-0252.1>.
- , K. D. Zaba, R. E. Todd, and R. E. Davis, 2017: A climatology of the California Current System from a network of underwater gliders. *Prog. Oceanogr.*, **154**, 64–106, <https://doi.org/10.1016/j.pocean.2017.03.002>.
- Sherman, J., R. E. Davis, W. B. Owens, and J. Valdes, 2001: The autonomous underwater glider “Spray.” *IEEE J. Oceanic Eng.*, **26**, 437–446, <https://doi.org/10.1109/48.972076>.
- Todd, R. E., D. L. Rudnick, and R. E. Davis, 2009: Monitoring the greater San Pedro Bay region using autonomous underwater gliders during fall of 2006. *J. Geophys. Res.*, **114**, C06001, <https://doi.org/10.1029/2008JC005086>.
- , —, M. R. Mazloff, R. E. Davis, and B. D. Cornuelle, 2011: Poleward flows in the southern California Current System: Glider observations and numerical simulation. *J. Geophys. Res.*, **116**, C02026, <https://doi.org/10.1029/2010JC006536>.
- , —, J. T. Sherman, W. B. Owens, and L. George, 2017: Absolute velocity estimates from autonomous underwater gliders equipped with Doppler current profilers. *J. Atmos. Oceanic Technol.*, **34**, 309–333, <https://doi.org/10.1175/JTECH-D-16-0156.1>.